C. R. Mecanique 343 (2015) 700–711

Contents lists available at ScienceDirect

Comptes Rendus Mecanique

www.sciencedirect.com

Acoustic metamaterials and phononic crystals

Torsional topology and fermion-like behavior of elastic waves in phononic structures

Pierre A. Deymier *, Keith Runge, Nick Swinteck, Krishna Muralidharan

Department of Materials Science and Engineering, University of Arizona, Tucson, AZ 85721, USA

ARTICLE INFO

Article history:
Received 15 January 2015
Accepted 15 May 2015
Available online 27 July 2015

Keywords:
Phonons
Fermions
Topological elastic waves
Phononic structure

ABSTRACT

A one-dimensional block-spring model that supports rotational waves is analyzed within Dirac formalism. We show that the wave functions possess a spinor and a spatio-temporal part. The spinor part leads to a non-conventional torsional topology of the wave function. In the long-wavelength limit, field theoretical methods are used to demonstrate that rotational phonons can exhibit fermion-like behavior. Subsequently, we illustrate how information can be encoded in the spinor-part of the wave function by controlling the phonon wave phase.

1. Introduction

Our understanding of elastic waves has been nourished essentially by the simple paradigm of the plane wave and its periodic counterpart (the Bloch wave) in periodic media. Significant progress has been achieved in unraveling the behavior of elastic waves in phononic crystals and acoustic metamaterials [1]. However, most of this progress has been achieved through exploration of the geometrical complexity of these media. Inspired by the discovery of topological insulators for which the electronic wave function is supported in momentum space by manifolds with non-conventional topologies [2], recent studies have shown the possibility of achieving electromagnetic waves [3,4] and acoustic waves with non-conventional topologies [5,6]. In the present paper, we investigate the properties of wave functions in phononic structures supporting rotational waves which can exhibit wave functions that take the form of spinors [7]. The non-conventional torsional topology of the wave function of elastic waves with spinor characteristics leads to a constraint on the wave function reminiscent of the Pauli-exclusion principle. This type of constraint introduces the notion of fermion-like behavior of elastic waves. Topological constraints on elastic waves promises to offer unique, robust designs and new device functionalities to phononic systems by providing immunity to performance degradation caused by imperfections [8,9] or information coding and processing in the phase of the waves.

In reference [7], we reported on an investigation of a 2D PC constituted of stiff polymer inclusions in a soft elastomer matrix. The 2D PC composed of a square array of polystyrene (PS) inclusions in a polydimethylsiloxane (PDMS) elastomer matrix was shown to support rotational waves. Of particular interest were modes where the PS inclusions and the region of the matrix separated by the inclusions rotate out of phase but also in phase. Following Peng et al. [10], who demonstrated that a 1D lumped mass model could be used to describe rotational modes in a 2D PC, we introduced a 1D mass spring phononic structure that could also support rotational waves. The 1D model was used to reproduce the dispersion relations of the 2D system in a certain range. We then showed within Dirac's formalism that the wave function for rotational waves possessed a spinor-part and a spatio-temporal part.

* Corresponding author.
E-mail address: deymier@email.arizona.edu (P.A. Deymier).

http://dx.doi.org/10.1016/j.crme.2015.07.003
1631-0721/

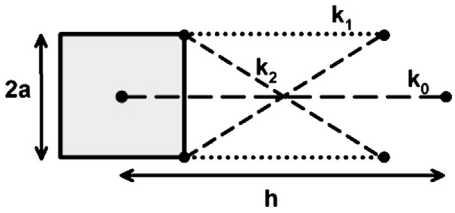

Fig. 1. Schematic illustration of a discrete micromechanics model that supports rotational waves. Unit cell of a monoblock model with elements (blocks) connected by three types of harmonic springs (spring constants k_0, k_1, and k_2). Each element possesses translational longitudinal (u), shear (v) and rotational (φ) degrees of freedom.

In the present paper, we investigate the geometric topology of the spinor-part of the wave function. We show that the spinor-part imparts a non-conventional topology to the wave function. In particular, the spinor part of the elastic wave function is supported in momentum space by a manifold with torsional topology. Furthermore, in the long-wavelength limit of the 1D model, we integrate the concepts of phononic structures that support rotational waves with that of a Dirac representation of elastic waves within a field theoretical framework. This leads to the observation of fermion-like behavior resulting from the spinor part of the wave function. In particular within the context of a "second quantization" of the rotational waves, we show that the properties of their associated spinor lead to anticommutation rules for the creation and annihilation operators.

After showing the possibility of fermion-like constraints on the elastic waves, a second question related to the more practical aspect of this behavior is also posed: what are the implications of fermion-like phonon behavior? A partial answer to that question is offered by introducing the concept of phase control of phonons through the specificity of their fermion character. To that effect, we introduce the concept of a phononic structure-based φ(phase)-bit. We demonstrate that one can operate on the φ-bit through the structure's physical parameters to transform the spinor state of the wave function. More specifically, one can operate on and measure the spinor state of phonons replicating known operations that are more commonly executed on fermions states like spins.

This paper is organized as follows: in Section 2, we describe the 1D discrete mass-spring model that supports rotational modes. This model forms the foundation of the development of a field theoretical representation of rotational modes in phononic structures. The wave equation associated with that model is shown to be isomorphic to the Klein–Gordon equation. That equation is therefore factored using Dirac formalism. We obtain the wave functions and investigate their non-conventional topology in momentum (k) space. In Section 3, we use quantum field theoretic methodologies to analyze the properties of the wave functions in the long-wavelength limit. In particular we find constraints on the wave function reminiscent of fermion-like behavior. An application of these findings to the encoding and processing of information in the wave function is introduced in Section 4. Finally conclusions are drawn in Section 5.

2. Nonconventional topology of rotational waves in phononic crystals

2.1. One-dimensional discrete micromechanics model

Here, we describe a 1D mass-spring model that was shown in reference [7] to reproduce the dispersion relations of a 2D phonon crystal that supports rotational waves. This model is based on a discrete linear one-dimensional micromechanics model that includes longitudinal, shear and rotational degrees of freedom [11,12]. This 1D discrete lattice model consists of an infinite chain of square block elements connected with multiple harmonic springs. Each element in the model is considered to have two translational degrees of freedom (displacement in the x and y directions) and one rotational degree of freedom (rotation about an axis perpendicular to the xy-plane). Fig. 1 shows the repeatable unit cells for a monoblock lattice models with periodicity (h).

Three different harmonic springs (spring constants k_0, k_1, and k_2) connect different parts of the block elements. The element in Fig. 1 has mass (m) and moment of inertia (I). The block constituting the nth unit cell has x-displacement (u_n), y-displacement (v_n) and rotation component (φ_n). u_n and v_n represent displacements associated with longitudinal and transverse vibrations, respectively. The potential energy associated with the elastic connections of elements (n) and ($n+1$) in the monoblock chain is written as follows:

$$E_{n,n+1} = \frac{1}{2}K_0(u_{n+1}-u_n)^2 + \frac{1}{2}K_1\left[(v_{n+1}-v_n) + \frac{h}{2}(\varphi_{n+1}+\varphi_n)\right]^2 + \frac{1}{2}K_2(\varphi_{n+1}-\varphi_n)^2 \tag{1}$$

where $K_0 = (\frac{k_0}{h^2} + \frac{2k_1}{l^2} + \frac{2k_2 l^2}{l_d^4})$, $K_1 = (\frac{2k_2(2a)^2}{l_d^4})$, $K_2 = (\frac{2a^2k_1}{l^2})$, $l = h-(2a)$, $l_d = \sqrt{(l^2+(2a)^2)}$. Accordingly, the equations of motion for the element in the nth unit cell of the monoblock lattice are written as:

$$m\frac{\mathrm{d}^2u_n}{\mathrm{d}t^2} = K_0(u_{n+1}-2u_n+u_{n-1}) \tag{2}$$

$$m\frac{\mathrm{d}^2 v_n}{\mathrm{d}t^2} = K_1(v_{n+1} - 2v_n + v_{n-1}) + \frac{hK_1}{2}(\varphi_{n+1} - \varphi_{n-1}) \tag{3}$$

$$I\frac{\mathrm{d}^2 \varphi_n}{\mathrm{d}t^2} = K_2(\varphi_{n+1} - 2\varphi_n + \varphi_{n-1}) + \frac{hK_1}{2}(v_{n-1} - v_{n+1}) - \frac{h^2K_1}{4}(\varphi_{n+1} + 2\varphi_n + \varphi_{n-1}) \tag{4}$$

The band structure of such a lattice would contain three bands corresponding to the three degrees of freedom (u, v, and φ). However, for the sake of simplicity, we now restrict this model to the propagation of rotational waves by allowing only rotation of the blocks about their center of mass and by constraining shear and longitudinal displacements in the lattice. The equation of motion associated with the rotational degrees of freedom (equation (4)) then takes the simpler general form:

$$I\frac{\partial^2 \varphi_n}{\partial t^2} = K_1'(\varphi_{n+1} - 2\varphi_n + \varphi_{n-1}) - K_2'\varphi_n \tag{5}$$

$K_1' = K_2 - \frac{h^2K_1}{4}$, and $K_2' = h^2K_1$. Dividing the equation by I yields our rotational wave equation:

$$\frac{\partial^2 \varphi_n}{\partial t^2} - \beta^2(\varphi_{n+1} - 2\varphi_n + \varphi_{n-1}) + \alpha^2\varphi_n = 0 \tag{6}$$

with $\beta^2 = \frac{K_1'}{I}$ and $\alpha^2 = \frac{K_2'}{I}$.

Equation (6) takes the form of the discrete Klein–Gordon equation. Equation (6) involves the second derivatives with respect to continuous time and the discrete second derivative with respect to position of the angular degree of freedom. Here, following the approach of Dirac in linearizing the relativistic Klein–Gordon equation, we wish to derive a wave equation in terms of first order spatial and temporal derivatives. To do this we need to rewrite the Laplacian, $\Delta\varphi_n = \varphi_{n+1} - 2\varphi_n + \varphi_{n-1}$, in a "square root" form: $\Delta\varphi_n = D(D\varphi_n)$. This can be done exactly by introducing the following first order differential operator:

$$D = \boldsymbol{e_1}\Delta^+ + \boldsymbol{e_2}\Delta^- = \begin{pmatrix} 0 & 1 \\ 0 & 0 \end{pmatrix}\Delta^+ + \begin{pmatrix} 0 & 0 \\ 1 & 0 \end{pmatrix}\Delta^- \tag{7}$$

In equation (7), $\Delta^+\varphi_n = \varphi_{n+1} - \varphi_n$ and $\Delta^-\varphi_n = \varphi_n - \varphi_{n-1}$ are the forward and backward finite differences acting now on a two-vector. The 2×2 matrices $\boldsymbol{e_1}$ and $\boldsymbol{e_2}$ satisfy the conditions $\boldsymbol{e_1}\boldsymbol{e_1} = \boldsymbol{e_2}\boldsymbol{e_2} = 0$ and $\boldsymbol{e_1}\boldsymbol{e_2} + \boldsymbol{e_2}\boldsymbol{e_1} = \boldsymbol{I}$ with $\boldsymbol{I}$ representing the 2×2 identity matrix. This formalism permits the exact and formal definition of the "square root" of the discrete Laplacian.

The Dirac-like equation for rotational waves corresponding to case I, then takes the form:

$$\left[\boldsymbol{\sigma_x}\otimes\boldsymbol{I}\frac{\partial}{\partial t} + \mathrm{i}\beta\boldsymbol{\sigma_y}\otimes\left\{\boldsymbol{e_1}\Delta^+ + \boldsymbol{e_2}\Delta^-\right\} \pm \mathrm{i}\alpha\boldsymbol{I}\otimes\boldsymbol{I}\right]\psi = 0 \tag{8}$$

where $\boldsymbol{\sigma_x}$ and $\boldsymbol{\sigma_y}$ are the 2×2 Pauli matrices: $\left(\begin{smallmatrix} 0 & 1 \\ 1 & 0 \end{smallmatrix}\right)$ and $\left(\begin{smallmatrix} 0 & -\mathrm{i} \\ \mathrm{i} & 0 \end{smallmatrix}\right)$, respectively. The parameter α plays the role of mass in the relativistic Dirac equation. Applying the outer product $\otimes$ leads to 4×4 matrices and ψ is a four-vector: $\psi = \begin{pmatrix} \psi_{1n} \\ \psi_{2n} \\ \psi_{3n} \\ \psi_{4n} \end{pmatrix}$. This four-component representation is the consequence of the discrete nature of the Laplacian. In contrast, with a continuous Laplacian, there is no distinction between forward and backward derivatives and one would only need to use a two-component representation. This is the case in the long-wavelength limit of Section 3. In this limit, having a two-component spinor indicates that there is a coupling between waves propagating in opposite directions (positive or negative) along the chain of blocks. When considering the short-wavelength four-component spinor solution, the first two components represent propagation of waves in the positive direction and the next two components propagation in the negative direction. The two components for the positive direction and the two components from the negative directions reflect a lifting of degeneracy due to asymmetry of the forward and backward finite different in the discrete Dirac equation. The solutions of equations (8) are automatically solutions of equation (6), but the converse is not true. As will be seen later, the directions of propagation of the wave are expressed separately in the Dirac wave function. The $\pm$ in equation (8) corresponds to choices of the sign of the parameter α (i.e. choice of positive or negative "mass" in Dirac's formalism). Let us first seek solutions of equation (8) with the negative value. Equation (8) becomes:

$$\left[\boldsymbol{C}\frac{\partial}{\partial t} + \beta\left\{\boldsymbol{A}\Delta^+ + \boldsymbol{B}\Delta^-\right\} - \mathrm{i}\alpha\boldsymbol{I}\right]\psi = 0 \tag{9}$$

$\boldsymbol{C}$, $\boldsymbol{A}$, $\boldsymbol{B}$, and $\boldsymbol{I}$ are the 4×4 matrices:

$$\begin{pmatrix} 0 & 0 & 1 & 0 \\ 0 & 0 & 0 & 1 \\ 1 & 0 & 0 & 0 \\ 0 & 1 & 0 & 0 \end{pmatrix}, \quad \begin{pmatrix} 0 & 0 & 0 & 1 \\ 0 & 0 & 0 & 0 \\ 0 & -1 & 0 & 0 \\ 0 & 0 & 0 & 0 \end{pmatrix}, \quad \begin{pmatrix} 0 & 0 & 0 & 0 \\ 0 & 0 & 1 & 0 \\ 0 & 0 & 0 & 0 \\ -1 & 0 & 0 & 0 \end{pmatrix}, \quad \begin{pmatrix} 1 & 0 & 0 & 0 \\ 0 & 1 & 0 & 0 \\ 0 & 0 & 1 & 0 \\ 0 & 0 & 0 & 1 \end{pmatrix}$$

It is easily verifiable that $CC = I$, $AA = BB = 0$, $AB + BA = -I$, and $C(A\Delta^+ + B\Delta^-) + (A\Delta^+ + B\Delta^-)C = 0$, which are the conditions necessary to recover the wave equation (6) by applying the operator in equation (9) twice (with appropriate $\pm$ sign). Equation (9) is the basis for our discussion of rotational waves with non-trivial topologies in phononic structures.

Seeking solutions in the form of plane waves, $\psi_{jn} = a_j e^{-i\omega t} e^{iknh}$ with $j = 1, 2, 3, 4$. ω and k are the angular frequency and wavenumber, respectively. We remind the reader that "h" is the spacing distance between blocks. Equation (9) yields the system of equations:

$$\begin{cases} -i\alpha a_1 - i\omega a_3 + \beta(e^{ikh} - 1)a_4 = 0 \\ -i\alpha a_2 + \beta(1 - e^{-ikh})a_3 - i\omega a_4 = 0 \\ -i\omega a_1 - \beta(e^{ikh} - 1)a_2 - i\alpha a_3 = 0 \\ -\beta(1 - e^{-ikh})a_1 - i\omega a_2 - i\alpha a_4 = 0 \end{cases} \tag{10}$$

This system of equation admits two doubly degenerate eigenvalues:

$$\omega = \pm\sqrt{\alpha^2 - \beta^2\left(e^{ikh} - 1\right)\left(1 - e^{-ikh}\right)} = \pm\sqrt{\alpha^2 + 4\beta^2 \sin^2\frac{kh}{2}} \tag{11}$$

The negative frequency can be interpreted physically as follows [13]. Since the angular field ought to be a real-valued quantity, it can be written as the sum of a complex term and its complex conjugate. The negative frequency is associated with the complex conjugate term. The rotational mode at the origin, $k = 0$, has a finite frequency. We note that equation (11) gives two branches with positive and negative frequencies that do not intersect at the origin unless $\alpha = 0$. The dispersion relations are periodic and defined in the first Brillouin zone: $k \in [-\frac{\pi}{h}, \frac{\pi}{h}]$. Choosing the positive or negative branches of the dispersion relations, we determine the four eigenvectors:

$$\psi_1^{\pm} = \begin{pmatrix} a_1 \\ a_2 \\ a_3 \\ a_4 \end{pmatrix} e^{-i\omega t} e^{iknh} = a_0 \begin{pmatrix} ie^{+i\frac{kh}{4}}(\alpha - \beta(e^{i\frac{kh}{2}} - e^{-i\frac{kh}{2}})) \\ \mp e^{-i\frac{kh}{4}}\sqrt{\alpha^2 - \beta^2(e^{i\frac{kh}{2}} - e^{-i\frac{kh}{2}})^2} \\ \mp ie^{+i\frac{kh}{4}}\sqrt{\alpha^2 - \beta^2(e^{i\frac{kh}{2}} - e^{-i\frac{kh}{2}})^2} \\ e^{-i\frac{kh}{4}}(\alpha - \beta(e^{i\frac{kh}{2}} - e^{-i\frac{kh}{2}})) \end{pmatrix} e^{-i\omega t} e^{iknh} \tag{12a}$$

$$\psi_2^{\pm} = \begin{pmatrix} a_1 \\ a_2 \\ a_3 \\ a_4 \end{pmatrix} e^{-i\omega t} e^{iknh} = a_0 \begin{pmatrix} -ie^{+i\frac{kh}{4}}(\alpha + \beta(e^{i\frac{kh}{2}} - e^{-i\frac{kh}{2}})) \\ \mp e^{-i\frac{kh}{4}}\sqrt{\alpha^2 - \beta^2(e^{i\frac{kh}{2}} - e^{-i\frac{kh}{2}})^2} \\ \pm ie^{+i\frac{kh}{4}}\sqrt{\alpha^2 - \beta^2(e^{i\frac{kh}{2}} - e^{-i\frac{kh}{2}})^2} \\ e^{-i\frac{kh}{4}}(\alpha + \beta(e^{i\frac{kh}{2}} - e^{-i\frac{kh}{2}})) \end{pmatrix} e^{-i\omega t} e^{iknh} \tag{12b}$$

The upper signs in equations (12a) and (12b) correspond to the positive branch of the band structure ($\omega > 0$) and the lower signs to the negative branch ($\omega < 0$).

Similarly, we solve the equation:

$$\left[\boldsymbol{C}\frac{\partial}{\partial t} + \beta\left\{\boldsymbol{A}\Delta^+ + \boldsymbol{B}\Delta^-\right\} + i\alpha\boldsymbol{I}\right]\overline{\psi} = 0 \tag{13}$$

The operator in equation (13) is the complex conjugate of the operator in equation (9). So we seek solutions in the form of plane waves, $\overline{\psi}_{jn} = \bar{a}_j e^{i\omega t} e^{-iknh}$ with $j = 1, 2, 3, 4$. We find the four eigenvectors:

$$\overline{\psi}_1^{\pm} = \begin{pmatrix} \bar{a}_1 \\ \bar{a}_2 \\ \bar{a}_3 \\ \bar{a}_4 \end{pmatrix} e^{i\omega t} e^{-iknh} = a_0 \begin{pmatrix} ie^{-i\frac{kh}{4}}(\alpha - \beta(e^{i\frac{kh}{2}} - e^{-i\frac{kh}{2}})) \\ \mp e^{+i\frac{kh}{4}}\sqrt{\alpha^2 - \beta^2(e^{i\frac{kh}{2}} - e^{-i\frac{kh}{2}})^2} \\ \mp ie^{-i\frac{kh}{4}}\sqrt{\alpha^2 - \beta^2(e^{i\frac{kh}{2}} - e^{-i\frac{kh}{2}})^2} \\ e^{+i\frac{kh}{4}}(\alpha - \beta(e^{i\frac{kh}{2}} - e^{-i\frac{kh}{2}})) \end{pmatrix} e^{i\omega t} e^{-iknh} \tag{14a}$$

$$\overline{\psi}_2^{\pm} = \begin{pmatrix} \bar{a}_1 \\ \bar{a}_2 \\ \bar{a}_3 \\ \bar{a}_4 \end{pmatrix} e^{i\omega t} e^{-iknh} = a_0 \begin{pmatrix} -ie^{-i\frac{kh}{4}}(\alpha + \beta(e^{i\frac{kh}{2}} - e^{-i\frac{kh}{2}})) \\ \mp e^{+i\frac{kh}{4}}\sqrt{\alpha^2 - \beta^2(e^{i\frac{kh}{2}} - e^{-i\frac{kh}{2}})^2} \\ \pm ie^{-i\frac{kh}{4}}\sqrt{\alpha^2 - \beta^2(e^{i\frac{kh}{2}} - e^{-i\frac{kh}{2}})^2} \\ e^{+i\frac{kh}{4}}(\alpha + \beta(e^{i\frac{kh}{2}} - e^{-i\frac{kh}{2}})) \end{pmatrix} e^{i\omega t} e^{-iknh} \tag{14b}$$

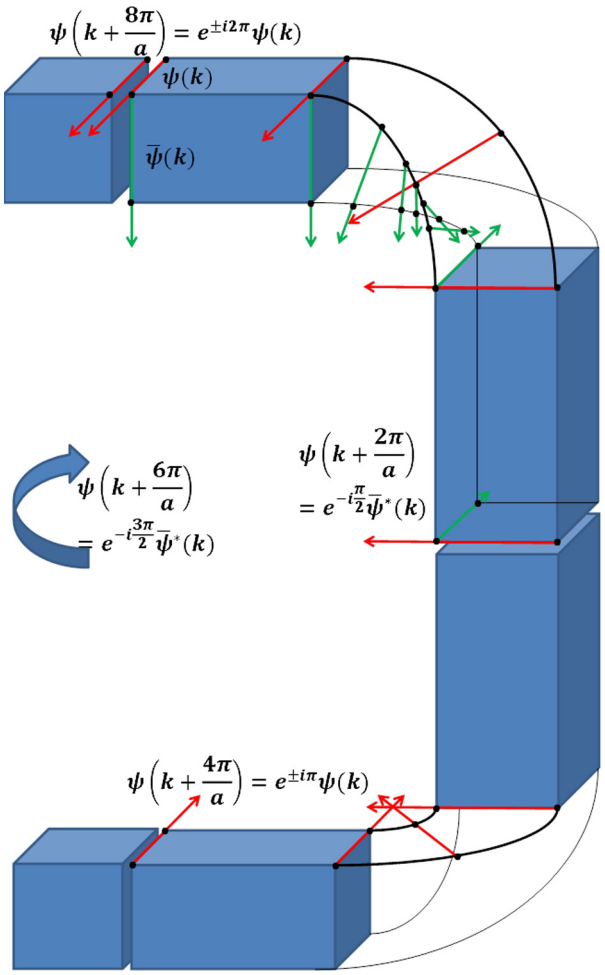

Fig. 2. (Color online.) Schematic illustration of the torsional topology of the wave function for rotational modes in k space. The wave functions are represented in the form of two orthogonal vector fields (red and green) supported by a square cross section torus manifold possessing four 90° twists. Parallel transport of the vector field on the manifold shows the topological properties of the wave function.

2.2. Non-conventional topology of rotational waves

Now, we investigate the topology in k space of the solutions given by equations (12a), (12b) and (14a), (14b). It is easy to show the following relations:

$$\psi^{\pm}_{1,2}\left(k+\frac{2\pi}{h}\right)=\mathrm{e}^{-\mathrm{i}\frac{\pi}{2}}\overline{\psi}^{*\pm}_{1,2}(k) \tag{15a}$$

$$\psi^{\pm}_{1,2}\left(k+\frac{4\pi}{h}\right)=\mathrm{e}^{-\mathrm{i}\pi}\psi^{\pm}_{1,2}(k) \tag{15b}$$

$$\psi^{\pm}_{1,2}\left(k+\frac{6\pi}{h}\right)=\mathrm{e}^{-\mathrm{i}\frac{3\pi}{2}}\overline{\psi}^{*\pm}_{1,2}(k) \tag{15c}$$

$$\psi^{\pm}_{1,2}\left(k+\frac{8\pi}{h}\right)=\mathrm{e}^{-\mathrm{i}2\pi}\psi^{\pm}_{1,2}(k) \tag{15d}$$

In equatons (15a)–(15d), the * symbol represents the complex conjugate. We also note that ψ and $\overline{\psi}$ are orthogonal and satisfy: $\overline{\psi}\psi=0$. The relations given by equaton (15) indicate that the wave function has a periodicity of $\frac{8\pi}{h}$. The topology of the wave function is more easily illustrated by considering the parallel transport of two orthogonal vector fields along a closed loop corresponding to $k\in[0,\frac{8\pi}{h}]$. The first vector field represents the wave function ψ and the second vector field the complex conjugate of $\overline{\psi}$. This non-conventional torsional topology is illustrated in Fig. 2 in the form of a torus with square cross section that exhibits four 90° twists. Starting at the top of the figure, the red arrow and green arrow represent

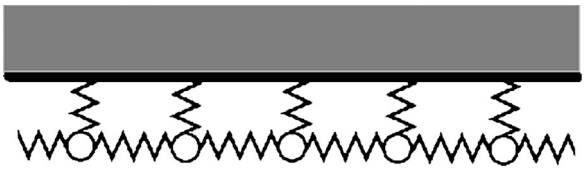

Fig. 3. Mass-spring system isomorphic to the block-spring system supporting rotational waves only.

the two orthogonal wave functions ψ and $\overline{\psi}$, respectively. The red arrow points in a direction perpendicular to the plane of the figure and the green arrow points in a direction within the plane of the figure. As the vector fields are transported along the first twist, the green arrow is now pointing in the plane of the figure and the green arrow becomes perpendicular to that plane, that is ψ turns into $\overline{\psi}$. The red arrow transported through the first twist is making now a right angle with the red arrow at the starting point. This means that the wave function ψ has accumulated a phase of $\frac{-\pi}{2}$. The process is repeated through the second twist. The red arrow transported through the second twist is now parallel to the red arrow at the origin but is pointing in the opposite direction and satisfies the condition: $\psi(k+\frac{4\pi}{h}) = -\psi(k)$. This means that the wave function ψ has accumulated a phase of $-\pi$. The vector fields can be transported through the third and fourth twists (not illustrated in the figure) to close the loop in k space and reach the starting point. At that point: $\psi(k+\frac{8\pi}{h}) = \psi(k)$.

The torsional topology of the wave function results from its spinor characteristics that endow it with fermion-like character. This character is analyzed in more details in the next section. To simplify the mathematics we consider only the long-wavelength limit.

3. Analysis of fermion-like behavior in the long-wavelength limit

3.1. Dirac equation in the long-wavelength limit

In the long-wavelength limit, $k \to 0$, equation (6) reduces to

$$\frac{\partial^2 \varphi}{\partial t^2} - \beta^2 \frac{\partial^2 \varphi}{\partial x^2} + \alpha^2 \varphi = 0 \tag{16}$$

We note that equation (16) is also that of a system composed of a one-dimensional harmonic chain composed of masses (m) connected to their nearest neighbors by springs with spring constant κ_1 and connected to a rigid substrate with a spring which constant is κ_2 (see Fig. 3). The relation between the equation of this spring-mass system and the rotational wave equation (16) is obtained by setting $\alpha^2 = \kappa_2/m$ and $\beta^2 = \kappa_1/m$. In the long-wavelength limit, this is a system composed of a string embedded in an elastic medium. The isomorphism between the block-spring system and the mass-spring model will be used in Section 4.

Equation (16) admits plane wave solutions with eigenvalues given by $\omega = \pm\sqrt{\alpha^2 + \beta^2 (kh)^2}$. At $k = 0$, the eigenmode with frequency $\omega = \alpha$ correspond to point B in Fig. 2. Note that to obtain the dispersion relation, we solved equation (16) by assuming plane wave solutions. These solutions correspond to traveling waves. However, the dispersion relation indicates that, for instance, at $k = 0$ the group velocity is zero, that is the eigenvector solution to (16) is a standing wave. Since a standing wave is the superposition of two waves traveling in opposite directions, equation (16) is unable to reveal the standing wave character of its solutions. Furthermore, the amplitude of the two oppositely traveling waves forming a standing wave have to be the same. Equation (16) does not impose any constraint on the amplitude of its plane wave solutions. For $k \neq 0$, the group velocity approaches the phase velocity only when $k \to \infty$, the solutions of equation (16) have mixed standing and traveling wave character. These solutions ought to be the superposition of waves traveling in opposite directions, whose amplitudes are not independent of each other, but are wavenumber dependent. It is these very observations that make the factorization of equation (16) into direction-specific equations necessary.

Equation (16) is isomorphic to the continuous relativistic Klein–Gordon equation. Here, again, following the approach of Dirac in linearizing the relativistic Klein–Gordon equation, we wish to derive a wave equation in terms of first order spatial and temporal derivatives:

$$\left[\boldsymbol{\sigma_x}\frac{\partial}{\partial t} + \mathrm{i}\beta\boldsymbol{\sigma_y}\frac{\partial}{\partial x} - \mathrm{i}\alpha\boldsymbol{I}\right]\psi = 0 \tag{17a}$$

$$\left[\boldsymbol{\sigma_x}\frac{\partial}{\partial t} + \mathrm{i}\beta\boldsymbol{\sigma_y}\frac{\partial}{\partial x} + \mathrm{i}\alpha\boldsymbol{I}\right]\overline{\psi} = 0 \tag{17b}$$

where $\boldsymbol{\sigma_x}$ and $\boldsymbol{\sigma_y}$ are the 2×2 Pauli matrices and $\boldsymbol{I}$ is the 2×2 identity matrix. We note that these equations are not self-dual. Taking the complex conjugate of equation (17a) results in equation (17b), indeed the first two terms are real and only the last term changes sign. In particular, this results from the negative sign of the second term in the Klein–Gordon equation (16), which requires the multiplicative imaginary number "i" in the second term of the Dirac-like equations (17a), (17b). Then $\overline{\psi} = \psi^*$. So while ψ is a solution of equation (17a), its complex conjugate is not a solution to (17a). $\overline{\psi}$ is

Table 1
Two by one spinor solutions of equations (17a) and (17b) for the different plane waveforms.

	$e^{+ikx}e^{+i\omega_k t}$	$e^{-ikx}e^{+i\omega_k t}$	$e^{+ikx}e^{-i\omega_k t}$	$e^{-ikx}e^{-i\omega_k t}$
ξ_k	$\begin{pmatrix}\sqrt{\omega+\beta kh}\\ \sqrt{\omega-\beta kh}\end{pmatrix}$	$\begin{pmatrix}\sqrt{\omega-\beta kh}\\ \sqrt{\omega+\beta kh}\end{pmatrix}$	$\begin{pmatrix}-\sqrt{\omega-\beta kh}\\ \sqrt{\omega+\beta kh}\end{pmatrix}$	$\begin{pmatrix}-\sqrt{\omega+\beta kh}\\ \sqrt{\omega-\beta kh}\end{pmatrix}$
$\bar{\xi}_k$	$\begin{pmatrix}\sqrt{\omega-\beta kh}\\ -\sqrt{\omega+\beta kh}\end{pmatrix}$	$\begin{pmatrix}\sqrt{\omega+\beta kh}\\ -\sqrt{\omega-\beta kh}\end{pmatrix}$	$\begin{pmatrix}\sqrt{\omega+\beta kh}\\ \sqrt{\omega-\beta kh}\end{pmatrix}$	$\begin{pmatrix}\sqrt{\omega-\beta kh}\\ \sqrt{\omega+\beta kh}\end{pmatrix}$

solution to equation (17b). In the language of Quantum Field Theory, ψ and $\overline{\psi}$ represent two different physical entities, namely "particles" and "antiparticles."

3.2. Lagrangian formalism

The Dirac-like equation (17a) derived in the previous section can be obtained from the Lagrangian:

$$L\left(\overline{\psi}, \frac{\partial\overline{\psi}}{\partial t}, \frac{\partial\overline{\psi}}{\partial x}\right) = \frac{\partial\overline{\psi}}{\partial t}\boldsymbol{\sigma_x}\psi + i\beta\frac{\partial\overline{\psi}}{\partial x}\boldsymbol{\sigma_y}\psi + i\alpha\overline{\psi}\boldsymbol{I}\psi \tag{18a}$$

In equation (18a), $\overline{\psi}$ is the Hermitian conjugate of ψ. The Lagrangian (18a) is Hermitian and its conjugate is given by:

$$\bar{L}\left(\psi, \frac{\partial\psi}{\partial t}, \frac{\partial\psi}{\partial x}\right) = \overline{\psi}\boldsymbol{\sigma_x}\frac{\partial\psi}{\partial t} + i\beta\overline{\psi}\boldsymbol{\sigma_y}\frac{\partial\psi}{\partial x} - i\alpha\psi\boldsymbol{I}\overline{\psi} \tag{18b}$$

The Lagrange's equation of motion for the field variables ψ is given by:

$$\frac{\partial}{\partial t}\left(\frac{\partial L}{\partial(\partial_t(\overline{\psi}))}\right) + \frac{\partial}{\partial x}\left(\frac{\partial L}{\partial(\partial_x\overline{\psi})}\right) - \frac{\partial L}{\partial(\overline{\psi})} = 0 \tag{19}$$

An equation of motion for the field $\overline{\psi}$ can also be obtain from equation (19) by replacing L by $\bar{L}$ and $\overline{\psi}$ by ψ. Using this approach, it is straightforward to recover equations (17a) and (17b).

3.3. Solutions of the long-wavelength Dirac equation

Having established the Dirac equation and its Hermitian conjugate (17a), (17b), we are now looking for solutions in the form of plane waves. Since these are matrix equations, we will seek solution that contains a spinor part (i.e. a two by one part matrix). We therefore write our solutions in the form: $\psi_k = \psi(k,\omega_k) = c_0\xi_k(k,\omega_k)e^{(\pm)i\omega_k t}e^{(\pm)ikx}$ and $\overline{\psi}_k = \overline{\psi}(k,\omega_k) = c_0\bar{\xi}_k(k,\omega_k)e^{(\pm)i\omega_k t}e^{(\pm)ikx}$ where ξ_k and $\bar{\xi}_k$ are two by one spinors. Inserting the various forms for these solutions in equations (17a), (17b) lead to the same eigenvalues that we obtained with the Klein–Gordon equation, namely: $\omega = \pm\sqrt{\alpha^2+\beta^2(kh)^2}$. The spinor part of the solutions for the different plane waves is summarized in Table 1.

The spinors in Table 1 are given to within any complex constant c_0.

Note that we will eventually promote the wave functions $\overline{\psi}$ and ψ to the rank of creation and annihilation operators, respectively, in Section 3.4.

We also note that if $\alpha = 0$, equation (17a) becomes: $[\boldsymbol{\sigma_x}\frac{\partial}{\partial t} + i\beta\boldsymbol{\sigma_y}\frac{\partial}{\partial x}]\psi = 0$. Using a plane wave solution with $\xi_k(k,\omega_k) = \binom{a_1}{a_2}$, this equation reduces to the system: $\begin{cases}(\omega-\beta kh)a_1 = 0\\ (\omega+\beta kh)a_2 = 0\end{cases}$. We obtain two solutions for the angular velocity of the plane wave, $\omega = \pm\beta kh$. These correspond to plane waves propagating in the positive and negative directions. In this case, the components of the two-spinor, a_1 and a_2 are now independent of each other and independent of the wavenumber. The amplitude of the plane wave propagating in the positive direction is independent of that of the wave propagating in the opposite direction. When $\alpha \neq 0$, from Table 1, we see that the components of the two-spinor are not independent of each other. This indicates that the directions of propagation are not independent of each other anymore. It is the parameter α that couples those directions.

3.4. Energy and anticommutation

Here we calculate the Hamiltonian density associated with the Lagrangian, $\bar{L}$. It is given by the Legendre transformation:

$$\overline{H} = \overline{\Pi}\frac{\partial\psi}{\partial t} - \bar{L} \tag{20}$$

where the momentum conjugate: $\overline{\Pi} = \frac{\partial\bar{L}}{\partial(\partial\psi/\partial t)} = \overline{\psi}\boldsymbol{\sigma_x}$. Inserting this expression in Equation (20) and using equation (18b), one obtains the Hamiltonian density:

$$\overline{H} = \overline{\psi}\boldsymbol{\sigma}_{\boldsymbol{x}}\frac{\partial\psi}{\partial t} \tag{21}$$

As mentioned earlier, we now promote the quantity ψ to an operator (we will use the same symbol ψ to represent the operator) and use a representation whereby the field ψ is expanded into plane waves and their complex conjugate:

$$\psi(x) = \sum_k \frac{1}{\sqrt{2\omega}}\left[a_k\xi_k e^{ikx}e^{-i\omega t} + a_k^*\xi_k^* e^{-ikx}e^{i\omega t}\right] \tag{22}$$

Similarly, we write the Hermitian conjugate of the ψ operator:

$$\overline{\psi}(x) = \sum_k \frac{1}{\sqrt{2\omega}}\left[\bar{a}_k\bar{\xi}_k e^{-ikx}e^{i\omega t} + \bar{a}_k^*\bar{\xi}_k^* e^{ikx}e^{-i\omega t}\right] \tag{23}$$

The quantities $\bar{a}_k$, $\bar{a}_k^*$, a_k, and a_k^* are creation and annihilation operators, respectively. Inserting equations (22) and (23) into equation (21) and integrating over all space results in

$$\begin{aligned} E = \int \mathrm{d}x\overline{H} = &\sum_k\sum_{k'}\frac{\bar{a}_{k'}}{\sqrt{2\omega'}}(-i\omega)\bar{\xi}_{k'}\boldsymbol{\sigma}_{\boldsymbol{x}}\xi_k\frac{a_k}{\sqrt{2\omega}}e^{-i(\omega-\omega')t}\int \mathrm{d}x\, e^{-i(k'-k)x} \\ &+\sum_k\sum_{k'}\frac{\bar{a}_{k'}}{\sqrt{2\omega'}}(i\omega)\bar{\xi}_{k'}\boldsymbol{\sigma}_{\boldsymbol{x}}\xi_k^*\frac{a_k^*}{\sqrt{2\omega}}e^{i(\omega+\omega')t}\int \mathrm{d}x\, e^{-i(k'+k)x} \\ &+\sum_k\sum_{k'}\frac{\bar{a}_{k'}^*}{\sqrt{2\omega'}}(-i\omega)\bar{\xi}_{k'}^*\boldsymbol{\sigma}_{\boldsymbol{x}}\xi_k\frac{a_k}{\sqrt{2\omega}}e^{-i(\omega+\omega')t}\int \mathrm{d}x\, e^{i(k'+k)x} \\ &+\sum_k\sum_{k'}\frac{\bar{a}_{k'}^*}{\sqrt{2\omega'}}(i\omega)\bar{\xi}_{k'}^*\boldsymbol{\sigma}_{\boldsymbol{x}}\xi_k^*\frac{a_k^*}{\sqrt{2\omega}}e^{-i(\omega'-\omega)t}\int \mathrm{d}x\, e^{-i(k-k')x} \end{aligned} \tag{24}$$

We now replace the spatial integrals in equation (24) by their respective delta functions, $\delta_{k',k}$, $\delta_{k',-k}$. Using Table 1, we can show that $\bar{\xi}_k\boldsymbol{\sigma}_{\boldsymbol{x}}\xi_k = \bar{\xi}_k^*\boldsymbol{\sigma}_{\boldsymbol{x}}\xi_k^* = 2\omega c_0^2$ and $\bar{\xi}_{-k}\boldsymbol{\sigma}_{\boldsymbol{x}}\xi_k^* = \bar{\xi}_{-k}^*\boldsymbol{\sigma}_{\boldsymbol{x}}\xi_k = 0$. Taking the constant $c_0^2 = -i$ to obtain an energy in the form of a real number, the energy of the system becomes:

$$E = \sum_k \omega\left(\bar{a}_k a_k - \bar{a}_k^* a_k^*\right) \tag{25}$$

To avoid the negative contribution to the energy in equation (25) and following the methods of quantum field theory, we need to impose anticommutation rules on the creation and annihilation operators, that is:

$$\{\bar{a}_k, a_{k'}\} = \bar{a}_k a_{k'} + a_{k'}\bar{a}_k = \delta_{k,k'} \tag{26}$$

With these anticommutation rules, the energy takes the form

$$E - E_0 = \sum_k \omega\left(\bar{a}_k a_k + a_k^*\bar{a}_k^*\right) \tag{27}$$

In equation (27), we have lumped the terms that arise from the delta function of equation (26) into a negative zero-point energy, $E_0 = -\sum_k \omega(k)$.

The anticommutation rules given by equation (26) also imply that $\bar{a}_k\bar{a}_k = 0$. This is Pauli's exclusion principle, stating that one cannot create more than one particle per state. The anticommutation rules indicate that the rotational modes have fermion character. How can these anticommutation rules be interpreted physically? The fields given by (22) and (23) are composed of forward and backward traveling waves whose relative amplitudes are determined solely by the spinor part of the wave function $\xi_k e^{ikx}e^{-i\omega t}$. If one tries to add an additional traveling component to one of the quasi-standing solution via the operator $a_k^*\bar{a}_k^*$, one would create a new state that could not be a solution of the Dirac equations (17a), (17b). Such a state is not allowed. This restriction provides a physical interpretation of Pauli's exclusion principle.

3.5. Number operators

In the previous sub-section, we have shown that the energy is an invariant. This invariant is the consequence of the time reversal symmetry of equations (17a) and (17b). There exist other symmetries. In particular the Dirac-like equations are invariant upon the transformation involving a phase shift. Here we show that as a consequence, the number operator:

$$N = \int \mathrm{d}x\overline{\psi}\sigma_x\psi \tag{28}$$

is also an invariant. First, we start from the field operator given by equation (22) and replace k by $-k$ in the second term of the summation. This leads to:

$$\psi(x) = \sum_k \frac{1}{\sqrt{2\omega}}\left[a_k\xi_k e^{ikx}e^{-i\omega t} + a^*_{-k}\xi^*_{-k}e^{ikx}e^{i\omega t}\right] = \sum_k \frac{1}{\sqrt{2\omega}}\left[a_k\xi_k e^{ikx}e^{-i\omega t} + b_k\eta_k e^{ikx}e^{i\omega t}\right] \tag{29}$$

Similarly, we rewrite the field

$$\overline{\psi}(x) = \sum_k \frac{1}{\sqrt{2\omega}}\left[\bar{a}_k\bar{\xi}_k e^{-ikx}e^{i\omega t} + \bar{a}^*_{-k}\bar{\xi}^*_{-k}e^{-ikx}e^{-i\omega t}\right] = \sum_k \frac{1}{\sqrt{2\omega}}\left[\bar{a}_k\bar{\xi}_k e^{-ikx}e^{i\omega t} + \bar{b}_k\bar{\eta}_k e^{-ikx}e^{-i\omega t}\right] \tag{30}$$

Inserting equations (29) and (30) into (28), and following the same approach as in Sub-section 3.4, we obtain:

$$N = \sum_k \frac{1}{2\omega}(\bar{a}_k a_k\bar{\xi}_k\boldsymbol{\sigma_x}\xi_k + \bar{b}_k b_k\bar{\eta}_k\boldsymbol{\sigma_x}\eta_k) \tag{31}$$

Using Table 1 for the spinors and their Hermitian conjugate, we obtain

$$N = \sum_k (\bar{a}_k a_k + \bar{b}_k b_k) \tag{32}$$

This is clearly an invariant. The operator $\bar{a}_k a_k$ counts the number of waves propagating in a given directions and $\bar{b}_k b_k$ correspond to the number of waves propagating in the opposite direction. Considering a field representation that includes only one type of plane wave and therefore, looking at the first term of equation (32), we define the operator:

$$N_k = \frac{1}{2\omega}\bar{a}_k a_k\bar{\xi}_k\boldsymbol{\sigma_x}\xi_k \tag{33}$$

We recall that $\bar{\xi}_k\boldsymbol{\sigma_x}\xi_k = 2\omega = \omega + \beta kh + \omega - \beta kh$. Note that here, we have renormalized the spinors with respect to the arbitrary complex constant c_0. The last equality suggests the introduction of direction switching operators $\boldsymbol{S}_+ = \frac{1}{2}(\boldsymbol{\sigma_x} + i\boldsymbol{\sigma_y}) = \left(\begin{smallmatrix}0 & 1\\ 0 & 0\end{smallmatrix}\right)$ and $\boldsymbol{S}_- = \frac{1}{2}(\boldsymbol{\sigma_x} - i\boldsymbol{\sigma_y}) = \left(\begin{smallmatrix}0 & 0\\ 1 & 0\end{smallmatrix}\right)$. These operators anticommute: $\boldsymbol{S}_+\boldsymbol{S}_- + \boldsymbol{S}_-\boldsymbol{S}_+ = \boldsymbol{I}$. Using this later relation, we reformulate equation (33) in the form:

$$N_k = \frac{1}{2\omega}\bar{a}_k a_k\bar{\xi}_k\boldsymbol{I}\boldsymbol{\sigma_x}\xi_k = \bar{a}_k a_k\bar{\xi}_k\left(\frac{1}{2\omega}S_+S_-\sigma_x + \frac{1}{2\omega}S_-S_+\sigma_x\right)\xi_k \tag{34}$$

The operator $\frac{1}{2\omega}S_+S_-\sigma_x$ defines the occupancy of one of the directions along the chain of mass and springs. Its eigenvalues are given by $n_k^+ = \bar{\xi}_k\frac{1}{2\omega}S_+S_-\sigma_x\xi_k = \frac{\omega+\beta kh}{2\omega}$. The operator $\frac{1}{2\omega}S_-S_+\sigma_x$ defines the occupancy of the other opposite direction. Its eigenvalues are given by: $n_k^- = \bar{\xi}_k\frac{1}{2\omega}S_-S_+\sigma_x\xi_k = \frac{\omega-\beta kh}{2\omega}$. Considering the dispersion relation for the positive branch of the band structure, $\omega = +\sqrt{\alpha^2 + \beta^2(kh)^2}$, the eigenvalues, n_k^+ and n_k^-, can be rewritten in terms of the wave vector k only:

$$n_k^{\pm} = \frac{1}{2} \pm \frac{\beta kh/\alpha}{2\sqrt{1 + (\frac{\beta kh}{\alpha})^2}} \tag{35}$$

At the origin of the band structure, $k = 0$, and $n_k^+ = n_k^- = 1/2$. The direction occupancy is the same for the two opposite directions; hence the state of the system is described by a standing wave. For $k \to \infty$, $n_k^+ = 1$ and $n_k^- = 0$, and the phononic structure supports a pure traveling wave with only one direction favored. For finite k, one has the superposition of traveling and standing waves. By spanning the dispersion relation, one spans the "direction" states. One can quantify the "amount" of traveling wave character of the wave function with the quantity: $(n_k^+ - n_k^-)$. When expressed as a function of frequency, this quantity takes the functional form: $(n_k^+ - n_k^-) = \frac{\sqrt{\omega^2-\alpha^2}}{\omega}$. This clearly shows that the wave function character evolves from a pure standing wave at $\omega = \alpha$ to a pure traveling wave as the frequency increases to infinity.

The fermion-like behavior of the rotational wave opens up opportunities in the control of the direction of propagation of elastic waves. For instance, we have just seen that the two-spinor solution represents coupling between wave propagating in opposite directions. The spinor part of the wave function can be projected on the orthonormal basis $\left(\begin{smallmatrix}1\\0\end{smallmatrix}\right)$ and $\left(\begin{smallmatrix}0\\1\end{smallmatrix}\right)$ representing the possible directions of propagation of the wave. This enables us to encode information in the relative weight (phase) of the directions of propagation by controlling the wavenumber, k. This control will enable applications in the field of information processing. An example of these applications is given in the next section.

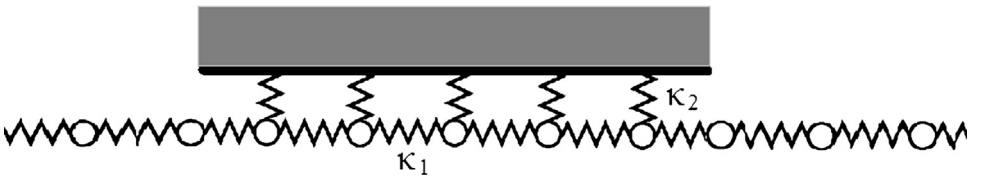

Fig. 4. Schematic illustration of the device composite system constituted of a segment of mass-spring system with fermion-like behavior sandwiched between two semi-infinite harmonic chains.

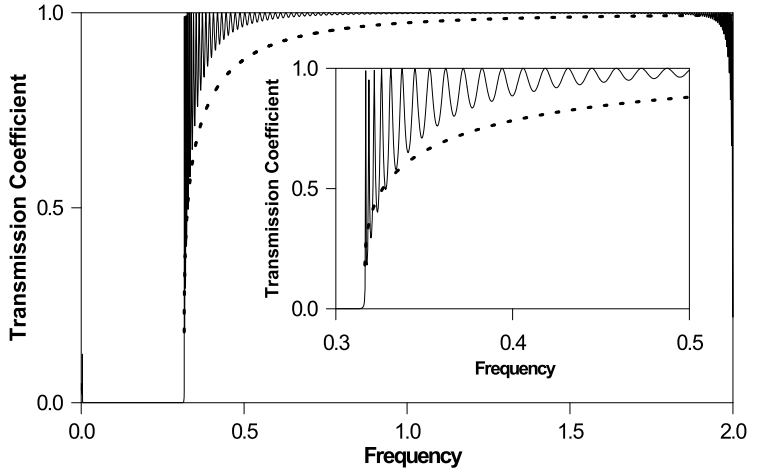

Fig. 5. Coefficient of transmission (solid line) of a plane wave launched in the right semi-infinite chain through the composite system illustrated in Fig. 4. The inset is a magnified region around the bottom of the positive branch of the band structure. The doted curve represents the traveling wave character of the wave function in the long-wavelength limit that is quantified by $(n_k^+ - n_k^-)^{0.5}$. See text for model parameters.

4. Applications to information processing

4.1. Phase control (φ)-bit

We now investigate how the properties of rotational waves and their fermion-like behavior can be used to encode and process information. For this, we use the isomorphism between the block-spring model and a mass-spring system introduced in Section 3 (see Fig. 3) and consider a device that is composed of a segment of mass-spring system isomorphic to the block-spring system supporting the rotational waves sandwiched between two semi-infinite harmonic chains (Fig. 4).

The number of masses in the central region of the sandwich is denoted N_c. We assume that all the masses, m, have the same value. We also assume that the spring constants of the semi-infinite regions are the same as the mass-to-mass spring constant, κ_1. The spring constant of the side springs is κ_2. We recall that these parameters map onto the parameters characterizing the rotational wave equation via the relations: $\alpha^2 = \kappa_2/m$ and $\beta^2 = \kappa_1/m$.

We are particularly interested in the transmission of plane waves launched from the left semi-infinite chain through the fermion-like segment. For this, we calculate the transmission coefficient of the composite system of Fig. 4. We employ the methods of the Interface Response Theory (IRT) [14]. The use of this method to calculate the transmission coefficient of infinite harmonic chains perturbed with harmonic finite side chains is detailed in [1].

We report in Fig. 5 the transmission coefficient as a function of frequency for a segment composed of $N_c = 80$ masses with side springs. We have chosen $m = 1$ and $\kappa_1 = 1$, that is $\beta^2 = 1$. The side springs have stiffness $\kappa_2 = 0.1$, i.e. $\alpha = 0.316$.

The transmission coefficient is zero for frequencies up to the value $\omega = \alpha = 0.316$. This zero transmission corresponds to the gap in the band structure of the rotational waves. Waves that are launched and propagate in the right semi-infinite harmonic chain cannot propagate through the central segment of the composite. Inside the passing band of the central segment, transmission occurs. The oscillatory nature of the transmission coefficient is due to the finite size and the discrete nature of the central segment. The frequency equal to 2 corresponds to the upper frequency of waves that can be supported by a discrete one-dimensional harmonic chain. The decrease of the transmission coefficient as the frequency of 2 is approached results from the curvature (zero group velocity) of the band of the one-dimensional harmonic chain. Therefore, one cannot establish a one-to-one correspondence between the long-wavelength limit result (dotted line) and the transmission through a discrete system. However, the general trend of an increase in transmission as the frequency increases from the bottom of the passing band of the central segment structure is representative of both the discrete and long-wavelength limit fermion-like behavior. The most important observation is that one can establish a one-to-one correspondence between a measurable scalar quantity: the transmission coefficient and the spinor characteristics of the wave that can be supported by the central

segment of the composite. For instance, for an incident wave $e^{ikx}e^{i\omega t}$ at $\omega=\alpha$ $(k=0)$, the transmission coefficient is zero and the spinor part of the wave function takes on the form: $\alpha\binom{1}{1}$. The components of the spinor vary monotonically as the frequency is increased (i.e. the wavenumber k is increased) until it takes a form approaching: $\sqrt{2\beta kh}\binom{1}{0}$. A similar tuning of the spinor part of the wave function can be achieved by fixing the frequency of the incident waves and varying the stiffness κ_2 (i.e. α) of the side springs relative to the stiffness of the 1D harmonic chain. From a practical point of view, this could be achieved by using springs composed of an elastic material whose stiffness is dependent on the magnitude of an externally applied electromagnetic wave (e.g., materials exhibiting photo-elastic effects [15]) or on an external magnetic field (e.g., magneto-elastic medium [16]). If we define a basis set $|0\rangle$ and $|1\rangle$ whose matrix representation takes the form of $\binom{1}{0}$ and $\binom{0}{1}$, one can create a superposition of state $u(\omega)|0\rangle+v(\omega)|1\rangle$ at fixed α or $u(\alpha)|0\rangle+v(\alpha)|1\rangle$ at fixed ω. Note that launching the incident wave from the right-hand side of the composite harmonic chain corresponds to an incident wave with $\omega<0$. In that case, for instance for $\omega=\alpha$ $(k=0)$, the spinor takes the value $\alpha\binom{-1}{1}$. This spinor is equivalent to the value $\alpha\binom{1}{-1}$ to within a factor of -1. Therefore, for a given incident wave of frequency ω, one can visualize the operation of tuning α, between zero and $\omega=\alpha$ as that of a Hadamard transformation. As seen previously, the Hadamard transformation can then be physically achieved by modulating the strength of an external stimulus such as the magnitude of an external field. In its matrix representation, the Hadamard transformation takes the form $\begin{pmatrix}1 & 1\\ 1 & -1\end{pmatrix}$ and transforms a wave launched from the left $\binom{1}{0}$ into the standing wave, whose spinor is proportional to $\binom{1}{1}$. It also transforms a wave propagating from the right $\binom{0}{1}$ into the standing wave whose spinor part is proportional to $\binom{1}{-1}$. The action of applying the Hadamard gate a second time is equivalent to detuning the parameter α between from $\omega=\alpha$ to zero. This transforms the states $\binom{1}{1}$ and $\binom{1}{-1}$ back into the traveling states $\binom{1}{0}$ and $\binom{0}{1}$. This transformation can be detected easily through the change in transmission from zero to 1. The control of the relative magnitude and sign of the spinor components of the wave function enables the encoding of information in the phase of the superposition of states. A system like that of Fig. 4 is what we define as a φ(phase)-bit. One can operate on the φ-bit through the system's physical parameter α via some external stimulus to transform the spinor state of the wave function. The Hadamard gate is an example of such an operation. The spinor state of the central segment of the φ-bit can be determined by measuring a single scalar quantity, namely the transmission coefficient. The question that arises now is that of the encoding of information on multiple φ-bits and the possibility of operating on them. This is addressed in the next section.

4.2. Operations on multiple φ-bits

Let us consider two φ-bits, $i=1,2$, each of which is prepared in the state: $|\xi_i\rangle=u(\alpha_i)|0\rangle+v(\alpha_i)|1\rangle$. The side springs in these two φ-bits are again composed of material whose stiffness is dependent on some external stimulus. Two external stimuli are applied on each φ-bits independently at this time. As seen in the previous section, this is achieved by launching a wave with frequency $\omega>\alpha_i$ to the right in each left semi-infinite chain. The transmission coefficient is measurable for each bit and takes on the value $T(\alpha_i)$. The two-bit system is in the initial product state: $|\xi_1\rangle\otimes|\xi_2\rangle$. One can now operate on this product state by defining a function $f(x)$ such that the product state becomes: $|\xi_1\rangle\otimes|f(\xi_1)\oplus\xi_2\rangle$. Because there is a one-to-one relation between $T(\alpha_1)$ and $|\xi_1\rangle$, this can be achieved by constructing a physical device that links the value of α_2 (i.e. the magnitude of the external stimulus acting of the second φ-bit) to that of the transmission coefficient of the first φ-bit. For instance, one can define $\alpha_2(T(\alpha_1))=f(T(\alpha_1))$. The new state of the second φ-bit will therefore take the form: $|\xi_2\rangle=u(\alpha_2(T(\alpha_1)))|0\rangle+v(\alpha_2(T(\alpha_1)))|1\rangle$. This procedure enables parallelism in the application of the operating function. This type of operation can then be applied straightforwardly to a system of N φ-bits, which could lead to parallel operations on the N-bit product state.

5. Conclusions

We investigate a 1D discrete block-spring model that supports rotational waves. This 1D discrete model is then analyzed within the Dirac's formalism. We have shown that rotational waves are characterized by wave functions that include a spinor part and a spatio-temporal part. The spinor part is related to the coupling between the senses of wave propagation. The spatio-temporal part of the wave function retains its plane-wave character. We have also investigated the topology of the wave function in k-space. We have shown that the wave function possesses a non-conventional torsional topology. The wave function is supported by a square cross section torus manifold exhibiting four 90° twists. This manifold has a periodicity of $\frac{8\pi}{h}$, where h is the periodicity of the 1D phononic structure.

The 1D system, in the long-wavelength limit, is shown to exhibit fermion character. The fermion-like behavior of phonons reported here arises from the coupling between waves propagating along the positive and negative directions and from the projection of the wave function on the orthogonal space of direction of propagation. This fermion behavior is associated with constraints reminiscent of Pauli's exclusion principle. The present exclusion principle is a reflection of the exact nature of the eigenvectors of the wave equation projected on the space of directions. The eigenvectors of the phononic structures presented here are not simply plane waves but a superposition of plane waves traveling in opposite directions. These superposition states can be visualized as quasi-standing waves possessing a standing wave character and a traveling wave contribution. For a given wave vector, it is the fixed ratio of the amplitudes of the standing wave component and of the traveling wave components that constrains wave propagation and imposes an exclusion principle-type restriction. That is,

one cannot superpose an additional traveling wave with the same wave vector without creating a new quasi-standing wave that is not solution of the wave equation.

We demonstrate one application of the properties of the wave function associated with its spinor character. Encoding of information in the elastic waves that are supported by the phononic structures described herein leads to the potential of operating simultaneously on the components of the spinor part of the wave functions. These operations act on the phase of states that can be written as superposition in a basis of pure forward or backward direction states. We call these φ-bits. The work presented here opens up opportunities in operating on the states of multiple φ-bits in a parallel fashion.

Finally, it is necessary to list some of the challenges one may encounter in realizing experimentally a device that exhibits the fermion-like behavior described in this paper. These challenges are associated with (a) the difficulties in exciting rotational elastic waves, (b) difficulties in exciting only pure rotational modes without exciting other longitudinal or transverse modes, (c) loss resulting from the intrinsic viscoelastic properties of the media constituting the device, and (d) loss resulting from geometrical non-linearity associated with rotational degrees of freedom.

References

[1] P.A. Deymier (Ed.), Acoustic Metamaterials and Phononic Crystals, Springer Series in Solid State Sciences, vol. 173, Springer, Heidelberg, Germany, 2013.
[2] M.Z. Hasan, C.L. Kane, Colloquium: topological insulators, Rev. Mod. Phys. 82 (2010) 3045.
[3] A.B. Khanikaev, S.H. Mousavi, W.-K. Tse, M. Kargarian, A.H. MacDonald, G. Shvets, Photonic topological insulators, Nat. Mater. 12 (2013) 233.
[4] M.C. Rechtsman, J.M. Zeuner, Y. Plotnik, Y. Lumer, D. Podolsky, F. Dreisow, S. Nolte, M. Sergev, A. Szameit, Photonic Floquet topological insulators, Nature 496 (2013) 196.
[5] E. Prodan, C. Prodan, Topological phonon modes and their role in dynamic instability of microtubules, Phys. Rev. Lett. 103 (2009) 248101.
[6] C.L. Kane, T.C. Lubensky, Topological boundary modes in isostatic lattices, Nat. Phys. 10 (2014) 39.
[7] P.A. Deymier, K. Runge, N. Swinteck, K. Muralidharan, Rotational modes in a phononic crystal with fermion-like behavior, J. Appl. Phys. 115 (2014) 163510.
[8] Z. Wang, Y. Chong, J.D. Joannopoulos, M. Soljacic, Observation of unidirectional backscattering-immune topological electromagnetic states, Nature 461 (2009) 772.
[9] N. Swinteck, S. Matsuo, K. Runge, J.O. Vasseur, P. Lucas, P.A. Deymier, Sound with a twist: bulk elastic waves with unidirectional backscattering-immune topological states, J. Appl. Phys. (2015), submitted for publication.
[10] P. Peng, J. Mei, Y. Wu, A lumped model for rotational modes in phononic crystals, Phys. Rev. B 86 (2012) 134304.
[11] A. Vasiliev, A. Miroshnichenko, M. Ruzzene, A discrete model and analysis of one-dimensional deformations in a structural interface with micro-rotations, Mech. Res. Commun. 37 (2010) 225–229.
[12] A. Vasiliev, A. Miroshnichenko, M. Ruzzene, Multifield model for Cosserat media, J. Mech. Mater. 3 (2008) 1365–1382.
[13] E. Rubino, J. McLenaghan, S.C. Kehr, F. Belgiorno, D. Townsend, S. Rohr, C.E. Kuklewicz, U. Leonhardt, F. Konig, D. Faccio, Negative-frequency resonant radiation, Phys. Rev. Lett. 108 (2012) 253901.
[14] L. Dobrzynski, Interface response theory of composite systems, Surf. Sci. 200 (1988) 435.
[15] J. Gump, I. Finckler, H. Xia, R. Sooryakumar, W.J. Bresser, P. Boolchand, Light-induced giant softening of network glasses observed near the mean-field rigidity transition, Phys. Rev. Lett. 92 (2004) 245501.
[16] O. Bou Matar, J.F. Robillard, J.O. Vasseur, A.-C. Hladky-Hennion, P.A. Deymier, P. Pernod, V. Preobrazhensky, Band gap tunability of magneto-elastic phononic crystal, J. Appl. Phys. 111 (2012) 054901.